Aerosol Science and Technology

ISSN: (Print) (Online) Journal homepage: https://www.tandfonline.com/loi/uast20

Water uptake and optical properties of mixed organic-inorganic particles

Lucy Nandy, Yu Yao, Zhonghua Zheng & Nicole Riemer

To cite this article: Lucy Nandy, Yu Yao, Zhonghua Zheng & Nicole Riemer (2021) Water uptake and optical properties of mixed organic-inorganic particles, Aerosol Science and Technology, 55:12, 1398-1413, DOI: 10.1080/02786826.2021.1966378

To link to this article: https://doi.org/10.1080/02786826.2021.1966378

AEROSOL SCIENCE AND TECHNOLOGY
2021, VOL. 55, NO. 12, 1398–1413
https://doi.org/10.1080/02786826.2021.1966378

Water uptake and optical properties of mixed organic-inorganic particles

Lucy Nandy[a]*, Yu Yao[a], Zhonghua Zheng[b]**, and Nicole Riemer[a]

[a]Department of Atmospheric Sciences, University of Illinois at Urbana-Champaign, Urbana, Illinois, USA; [b]Department of Civil and Environmental Engineering, University of Illinois at Urbana-Champaign, Urbana, Illinois, USA

ABSTRACT

Atmospheric aerosol particles are frequently mixtures of inorganic and organic species, both of which can contribute to aerosol water uptake and determine the particles' ability to scatter and absorb light. While water uptake of purely inorganic aerosol is well represented in current regional and global chemical transport models, it is challenging to represent it for particles that are mixtures of organic and inorganic species. Here we quantified the growth factor for aerosols that consist of mixed organic-inorganic particles using an accurate lattice-based adsorption isotherm model (Ad-iso) as a benchmark. We then determined the error in the growth factor and resulting optical properties for simplifying assumptions that are commonly made in current chemical transport models. The systems studied here are representative of ambient atmospheric aerosols, consisting of model water-soluble inorganic-organic mixtures, with and without a core of absorbing black carbon, under conditions of relative humidity larger than 85%. The assumption of completely neglecting the water uptake by organic components, for particles with an organic mass fraction of 50%, led to errors of up to 7% in growth factor and up to 3.5% in single scattering albedo. Larger errors occurred for larger organic mass fractions. Approximating the organic water uptake with a constant hygroscopicity parameter, for organic mass fractions between 45 and 65%, the errors remained within 3% for the growth factor and 0.6% for the single scattering albedo. For organic mass fractions smaller than 45% or larger than 65%, the errors increased up to 6% for the single scattering albedo. The magnitudes of these errors underscore the importance of considering organic/inorganic mixtures for estimating direct aerosol radiative forcing.

ARTICLE HISTORY
Received 11 May 2021
Accepted 28 July 2021

EDITOR
Jonathan Reid

1. Introduction

Aerosol particulate matter, or suspended solid or liquid particles in a gas, have diverse size distributions, chemical compositions, and physical properties that affect their impact on climate (Naik et al. 2013), air quality (von Schneidemesser et al. 2015) and human health (Heal, Kumar, and Harrison 2012; World Health Organization 2013). Fine mode particles (Aitken mode–less than 100 nm and accumulation mode–between 100 nm and 1 μm) are majorly composed of sulfate, ammonium, nitrate, dust, sea salt, organic carbon and black carbon.

The different chemical aerosol components become more internally mixed with gradual atmospheric processing during transport in the atmosphere, meaning that individual particles usually contain mixtures of organic and inorganic chemical species, including liquid water (Fuzzi et al. 2015; You, Renbaum-Wolff, and Bertram 2013; Pye et al. 2018). In these mixed particles, organic compounds influence the thermodynamic behavior including the water uptake of inorganic salts (Hodas et al. 2015; Estillore et al. 2017; Jing et al. 2016; Wong et al. 2014), and inorganic-organic chemical interactions in a particle are influenced by coexisting hygroscopic species (Peng et al. 2016). The resulting change in particle size is important to consider for the particles' scattering and absorption of sunlight (Fierce et al. 2016). This is particularly relevant when the particles are composed of black carbon (BC) coated with other inorganic-organic matter (Adachi and Buseck 2008; Bond, Habib, and Bergstrom 2006). Studies over the last two decades on mixed particles containing water-soluble coating (transparent materials) on BC have revealed that the absorption of the incoming solar radiation is enhanced in the visible spectrum (Xue et al. 2009;

CONTACT Lucy Nandy nandy.lucy@gmail.com Department of Chemistry, The Pennsylvania State University, 104 Chemistry Building, University Park, PA 16803, USA.
*Current affiliation: Department of Chemistry, The Pennsylvania State University, University Park, Pennsylvania, USA
**Current affiliation: Lamont-Doherty Earth Observatory of Columbia University, Palisades, New York, USA

Supplemental data for this article is available online at https://doi.org/10.1080/02786826.2021.1966378

Bond and Bergstrom 2006; Bond, Habib, and Bergstrom 2006; Zanatta et al. 2018; Wang et al. 2018; Cappa et al. 2012; Bond et al. 2013; Moosmüller, Chakrabarty, and Arnott 2009; Kou 1996; Knox et al. 2009; Fierce et al. 2016). Particles with water-soluble components (e.g., sulfates and organic carbon) scatter light depending on the aerosol water uptake at various relative humidities (RH) (Zieger et al. 2013; L. Zhang et al. 2015; Jefferson et al. 2017; Titos et al. 2016; Burgos et al. 2019). It is important to understand the optical properties of these mixtures to determine climate impacts at both regional and global scales (O'Brien et al. 2015; Bond and Bergstrom 2006; Moise, Flores, and Rudich 2015; Fierce et al. 2020).

To predict the gas-aerosol equilibrium partitioning in chemical transport models (CTMs), inorganic and organic compounds are usually treated in separate modules (Semeniuk and Dastoor 2020) within the host model. Such thermodynamic modules include ISORROPIA-II (Fountoukis and Nenes 2007), EQUISOLV II (Jacobson, Tabazadeh, and Turco 1996; Jacobson 1999), EQSAM (Metzger, Dentener, Pandis, et al. 2002; Metzger, Dentener, Krol, et al. 2002), SCAPE2 (Kim and Seinfeld 1995; Meng et al. 1995), and MOSAIC (Zaveri et al. 2008) for inorganic species, and MPMPO (Griffin et al. 2003) and SOA treatment in CMAQ v5.2 (Pye et al. 2017) for organic species. Common assumptions are that water uptake is only determined by the inorganic compounds, or the water uptake of organics is estimated by highly parameterized relationships assuming ideal solutions, e.g., using the kappa hygroscopicity parameter (Petters and Kreidenweis 2007). As a result, inaccurate aerosol water uptake estimations may lead to erroneous representations of particle growth which then propagate into the estimation of optical properties and radiative forcing. (Pye et al. 2018) studied the extent of water solubility of organic aerosol and suggested accounting for non-ideality in the model simulations of organic–inorganic water-uptake in the Community Multiscale Air Quality (CMAQv5) regional CTM (Pye et al. 2017; Appel et al. 2013). They found increased gas-to-particle partitioning for highly oxygenated compounds. Recently, a Binary Activity Thermodynamics (BAT) model has been developed to study nonideal water–organic interactions that may have a large impact on thermodynamic simulations within CTMs (Gorkowski, Preston, and Zuend 2019). It could be incorporated into 3-D transport models at reduced computational costs to evaluate water uptake and liquid-liquid phase separation.

The goal of this study is to quantify errors in aerosol water uptake and aerosol scattering and absorption when applying two commonly used simplifying assumptions about organic/inorganic/water mixtures, namely (1) assuming that the water uptake is solely determined by the inorganic compounds in the particles and (2) assuming that the water uptake by organic compounds can be parameterized by a constant hygroscopicity parameter, κ.

We use a recently developed adsorption isotherm model (Dutcher et al. 2013; Ohm et al. 2015; Nandy, Ohm, and Dutcher 2016; Nandy and Dutcher 2017) (Ad-iso) as a benchmark to calculate the non-reactive water uptake by fine aerosol particles composed of binary inorganic salts, ammonium sulfate and sodium chloride, and ternary water-soluble inorganic + organic compounds (ammonium sulfate/sodium chloride + glutaric acid/succinic acid/sucrose). The organic components, dicarboxylic acids, considered here are relevant as they are found in significant concentrations in the atmosphere (Kawamura and Ikushima 1993; Estillore et al. 2017), and play an important role in cloud condensation and ice nucleation processes (Rui and Ariya 2008; Yao et al. 2003). Current activity coefficient-based aerosol modules used in air quality and climate models are applied to only electrolyte containing non-dilute solutions with improved accuracy, failing to include the influence of mixed organic-inorganic constituents on the water uptake, whereas the adsorption model is applied to both electrolyte and organic containing solutions by deriving solute activities for both species using a single parameter statistical thermodynamic treatment.

The manuscript is organized as follows. Section 2 describes the methodology of water uptake calculations for the benchmark calculations and the two sensitivity cases. Section 3 presents particle growth and optical properties calculated by each model and discusses the impact of single scattering albedo variation on the direct aerosol radiative forcing uncertainty and sensitivity. Section 4 provides a summary and conclusions.

2. Methodology of water uptake calculations

2.1. Adsorption isotherm model for water uptake (Ad-iso)

The adsorption isotherm model (Nandy, Ohm, and Dutcher 2016; Nandy and Dutcher 2017), Ad-iso, is used here to calculate the aerosol water content for our reference case. Ad-iso was developed based on the lattice sorption of water molecules to a solute

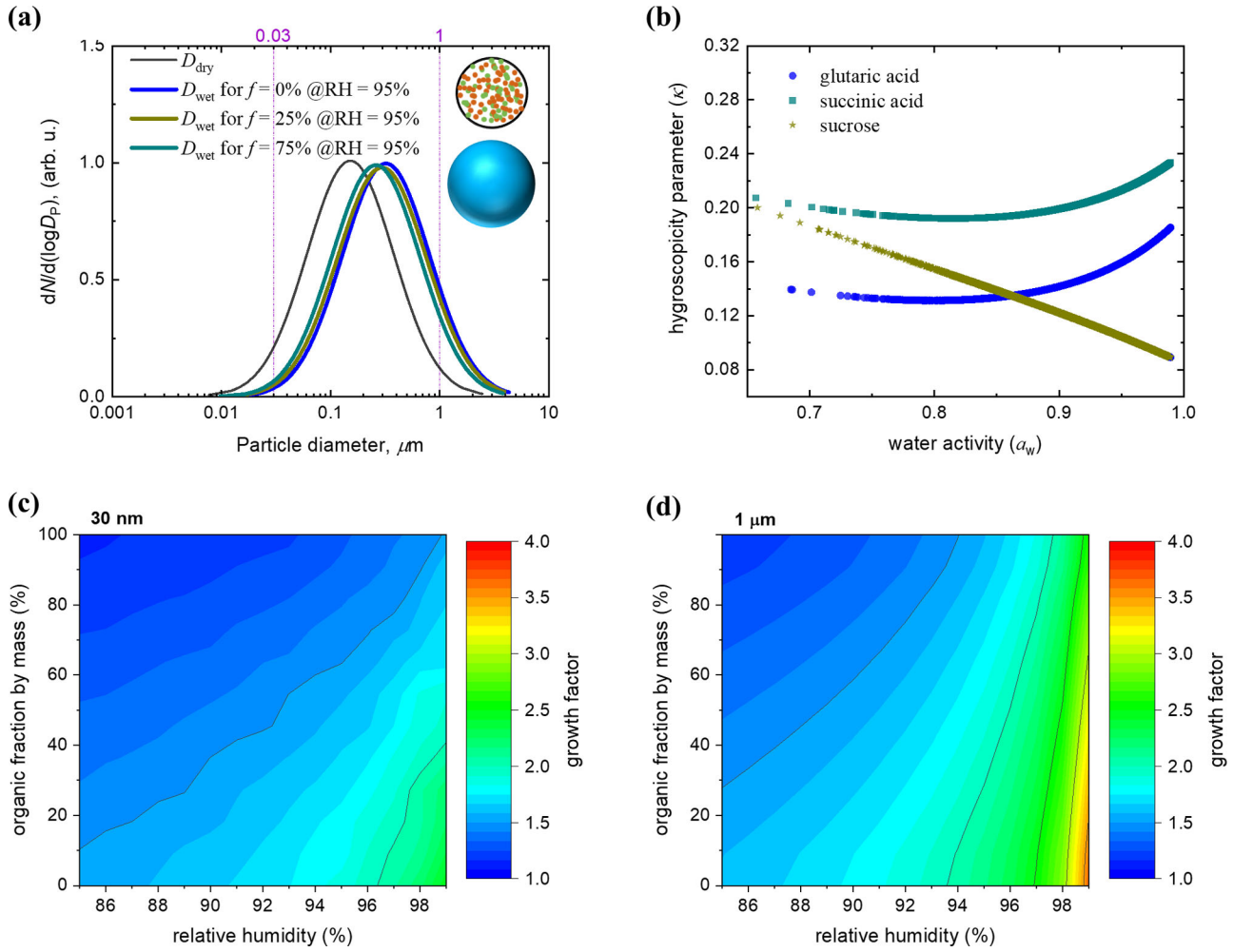

Figure 1. (a) Size distribution of an internally mixed aerosol containing ammonium sulfate and glutaric acid for fine dry particles and wet particles at RH = 95% (D_p = particle diameter). The inset spheres represent homogeneous dry and wet particles (not to scale). Inset: green spheres – organic molecules, orange spheres – inorganic molecules, blue sphere – homogeneously mixed inorganic, organic and water molecules. (b) Calculated hygroscopicity parameter, κ for single components glutaric acid, succinic acid and sucrose. (c, d) Hygroscopic growth factor of particles containing ammonium sulfate and glutaric acid for dry diameters (c) D_{dry} = 30 nm and (d) D_{dry} = 1 µm. Note that the contour plots in (c) and (d) only represent monodisperse particles and not the entire distribution as shown in (a); this is to illustrate an example of water uptake inhibition in smaller particles due to Kelvin effect. All plots in this figure are produced using Ad-iso model.

(Dutcher et al. 2011, 2012, 2013; Ohm et al. 2015; Nandy, Ohm, and Dutcher 2016; Nandy and Dutcher 2017). This thermodynamic model for aqueous particle phase is capable of determining the solute and water activities and concentrations for binary and multicomponent systems over the full RH range from 0 to 100%. The Ad-iso model for organic acids (Nandy, Ohm, and Dutcher 2016) and salts (Nandy and Dutcher 2017; Ohm et al. 2015) was developed and validated with available experimental water activity data from literature (see Figure S1 in online supplementary information [SI]). Figure S1a also compared Ad-iso with UNIFAC (Peng, Chan, and Chan 2001; Fredenslund, Jones, and Prausnitz 1975) and E-AIM (Wexler and Clegg 2002) showing greater accuracy over the entire solute concentration range. The Ad-iso model has been used to study hygroscopicity in dicarboxylic acids and amino acids (Marsh et al. 2017; Cai et al. 2015), pH in weak acids (Craig et al. 2017; Craig et al. 2018), and effect of viscosity on water-sucrose-maleic acid (Marshall et al. 2016, 2018) system. In this article, to estimate the mass of water uptake, a density model (Marshall et al. 2018; Laliberte and Cooper 2004) is combined because the Ad-iso model alone calculates the water content on a molality basis. The density model assumes ideal behavior in dilute solutions and iteratively calculates the solution density. This is in contrast to existing aerosol models, which calculate the mass of water by approximating the solution volume as the sum of the

dry solute volume and the solvent volume (here water), for simplicity. The ideal mixture density approximation at lower solute mass fractions less than 0.4 has been validated previously (Cai et al. 2016). Therefore, at RH > 85%, volume weighted average density calculations are acceptable. We have compared both methods and found errors to remain within 0.5%. The Ad-iso model is based on statistical mechanics of multilayer sorption and derives an expression relating water activity to solute molality as a function of difference in sorption energies (energy of bound water to the solute – energy of free water in the bulk) (Dutcher et al. 2011, 2013). The model inputs are RH (equivalent to water activity for bulk solutions at thermodynamic equilibrium) and molar ratio of solutes present in a particle; and the model outputs are, therefore, the solution concentration and thermodynamic activities of each solute. The sub-modules calculate the solution density and hygroscopicities with respect to water activity.

In previous studies, Ad-iso has been applied to particles larger than 100 nm so that the equilibrium vapor pressure was not significantly altered by the droplet surface curvature. Here we extended our analysis to particles smaller than 100 nm diameter where the Kelvin effect is significant. The κ-Köhler theory, described by Equations (1) and (2), were used to evaluate the water activity of the particle, a_w, as a_w is now not equal to RH/100 but instead related to each other by

$$\frac{\mathrm{RH}}{100\%} = a_w + \exp\left(\frac{2\nu_w\sigma_s}{RTD_{wet}}\right), \quad (1)$$

where ν_w is the molar volume of water (18 cm^3/mol), R is the universal gas constant, T is the temperature in K, D_{wet} is the wet particle diameter and σ_s is the surface tension of the solution particle with air interface. All diameters in this study are volume equivalent diameters. We used the surface tension of water, σ_w (72 mN/m), at 298.15 K for all systems in this article, rather than the surface tension of the solution σ_s. We confirmed with E-AIM (Wexler and Clegg 2002) that σ_w in place of σ_s only leads to negligible errors in the calculations of wet diameter (less than 1.3%) for the aqueous binary ammonium sulfate system and the relative humidity values considered in this article (RH larger than 85%). Equation (2) follows Petters and Kreidenweis parameterization (Petters and Kreidenweis 2007) to define a dimensionless hygroscopicity parameter, κ, described by

$$\frac{1}{a_w} = 1 + \kappa\frac{V_s}{V_w} \quad (2)$$

where V_s is the volume of the dry particle $\left(\frac{\pi}{6}D_{dry}{}^3\right)$, V_w is the volume of water in the wet particle and D_{dry} is the dry particle diameter. The wet diameter D_{wet} and a_w are related to the hygroscopicity of the solute components, which allows for the iteration of a_w, by using the volume-weighted hygroscopicity parameter, κ (Equation (3) in Section 2.3) as an initial value. An additional input in the Ad-iso model is now D_{dry} as defined in the setup of size distribution below. The iterated value of a_w takes the Kelvin effect into account, and therefore, κ values are re-calculated as a function of a_w for each single component.

The hygroscopic growth factor, gf $= \frac{D_{wet}}{D_{dry}}$, used in this article, is a result of water uptake by the soluble aerosol particles depending on the chemical composition, relative humidity and temperature, assuming a fully internally mixed aerosol. Dry fine particles (diameter, D_{dry} less than 2.5 µm) were considered with varied water-soluble organic/inorganic compositions. Assuming all components to be fully dissolved in water, the wet diameter was calculated for relative humidities (RH) 85% to 99%, and organic dry mass fractions (f) 0% to 95% to evaluate the impact of organic/inorganic mixtures on water uptake of particles. The wet size distributions for several cases of ammonium sulfate + glutaric acid mixtures estimated by the Ad-iso model are shown in Figure 1a, by calculating the water uptake and hence droplet growth for the particles of different sizes. As expected, increasing organic fraction inhibits water uptake (Wong et al. 2014). The aerosol population in Figure 1a follows a log-normal size distribution (total number concentration, $N = 10^5$ m^{-3}, geometric mean diameter, D_g = 0.17 µm, geometric standard deviation, σ_g = 2.4). We will use this size distribution in the remainder of the article as a representative example for our calculations, noting that the results remained qualitatively the same if the size distribution parameters were changed. The models used in this study assumed particles to be one liquid phase homogeneously mixed at 298.15 K, to estimate water uptake with varying relative humidities and organic mass fractions. We did not consider liquid-liquid phase separation and organic constituents that may act as surfactants (McFiggans et al. 2006) in this study. Each dry particle within the population was assumed to have the same chemical composition, as shown in Figure 1a.

Ad-iso was used as a benchmark in this study because it considers both inorganic and organic solutes taking up water from the ambient air, as well as

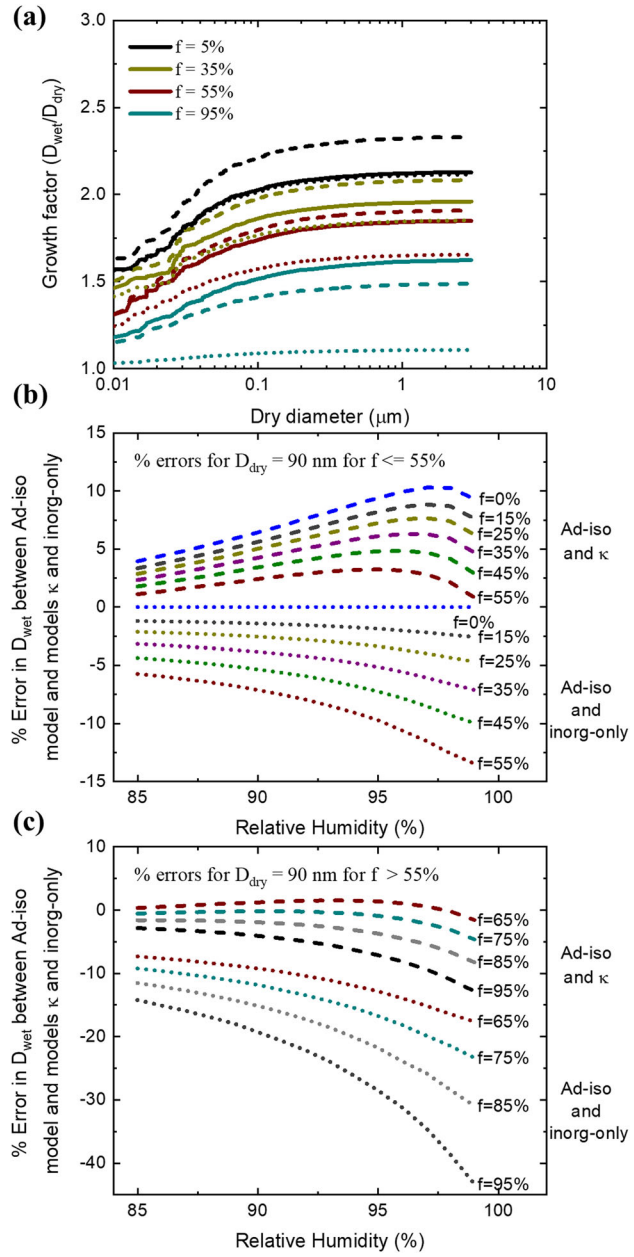

Figure 2. (a) Comparison of size-resolved hygroscopic growth factor particles containing ammonium sulfate and glutaric acid at RH = 95%. Lines: solid – Ad-iso model, dash – κ-model, dot – inorg-only model. Each colored set of lines has a fixed organic fraction. (b, c) Relative error in wet diameter of monodisperse particles of dry diameter (D_{dry}) 90 nm containing ammonium sulfate and glutaric acid; (b) 0% $\leq f \leq$ 55%; (c) $f >$ 55%. Lines: dash – error of κ-model, dot – error of inorg-only model.

a varying κ as a function of water activities (Figures 1b and S2). Figures 1c and d demonstrate that the particle growth was sensitive to particle size, e.g., the growth factor for a 30 nm particle showed growth inhibition compared to a bigger particle of 1 μm. This was due to the Kelvin effect. Figures 1c and d also demonstrate that droplet growth increased rapidly at higher relative humidities, and was inhibited with increasing organic fraction (Wong et al. 2014). The simplifying model assumptions that are compared with the Ad-iso reference case are described next.

2.2. Water uptake by inorganic components only ("inorg-only" model)

To calculate the water uptake for our case "inorg-only," we used the Ad-iso model assuming that only the inorganic component takes up water from the ambient air, and the organic component is not hygroscopic. To check the Ad-iso calculations, we compared the water uptake of pure ammonium sulfate with the results using PartMC-MOSAIC (Particle Monte Carlo; Model for Simulating Aerosol Interactions and Chemistry) (Riemer et al. 2009; Zaveri et al. 2008) by generating several monodisperse particle populations at different dry diameters consisting of ammonium sulfate at a prescribed relative humidity, with an abundance of NH_3 in the gas phase, and recorded the associated water uptake. Ad-iso and PartMC-MOSAIC give the same results, shown in Figure S3.

2.3. Water uptake by inorganic components and by organic components using κ-Köhler theory (κ model)

For the second comparison method "κ," the κ-Köhler theory (Petters and Kreidenweis 2007) was used to calculate the water uptake using Equation (2), where RH/100 is the saturation ratio over the solution droplet. A fixed hygroscopicity parameter, κ, which depends on the solute, was used to calculate the water content as in the Equation (2) in Section 2.1. For a multicomponent system, the κ value was calculated by the mixing rule given by

$$\kappa = \sum\nolimits_i \varepsilon_i \kappa_i \quad (3)$$

where ε is the dry component volume fraction, and i is the solute component. For calculations in this study, the hygroscopicity parameters for ammonium sulfate (AS) and sodium chloride (NaCl) were taken as 0.65 and 1.28, respectively, and for organic compounds as 0.1. The value of 0.1 for organic compounds represents a comparatively low value (Figure 1b), which follows κ measurements of secondary organic aerosols (SOA) reported to be 0.1 ± 0.04 in previous studies (Prenni et al. 2007; Asa-Awuku et al. 2010; Suda et al. 2012, 2014; Engelhart et al. 2008; Kuang et al. 2020). A kappa value of 0.1 is a typical value chosen for SOA in simplified models, e.g., in PartMC-MOSAIC.

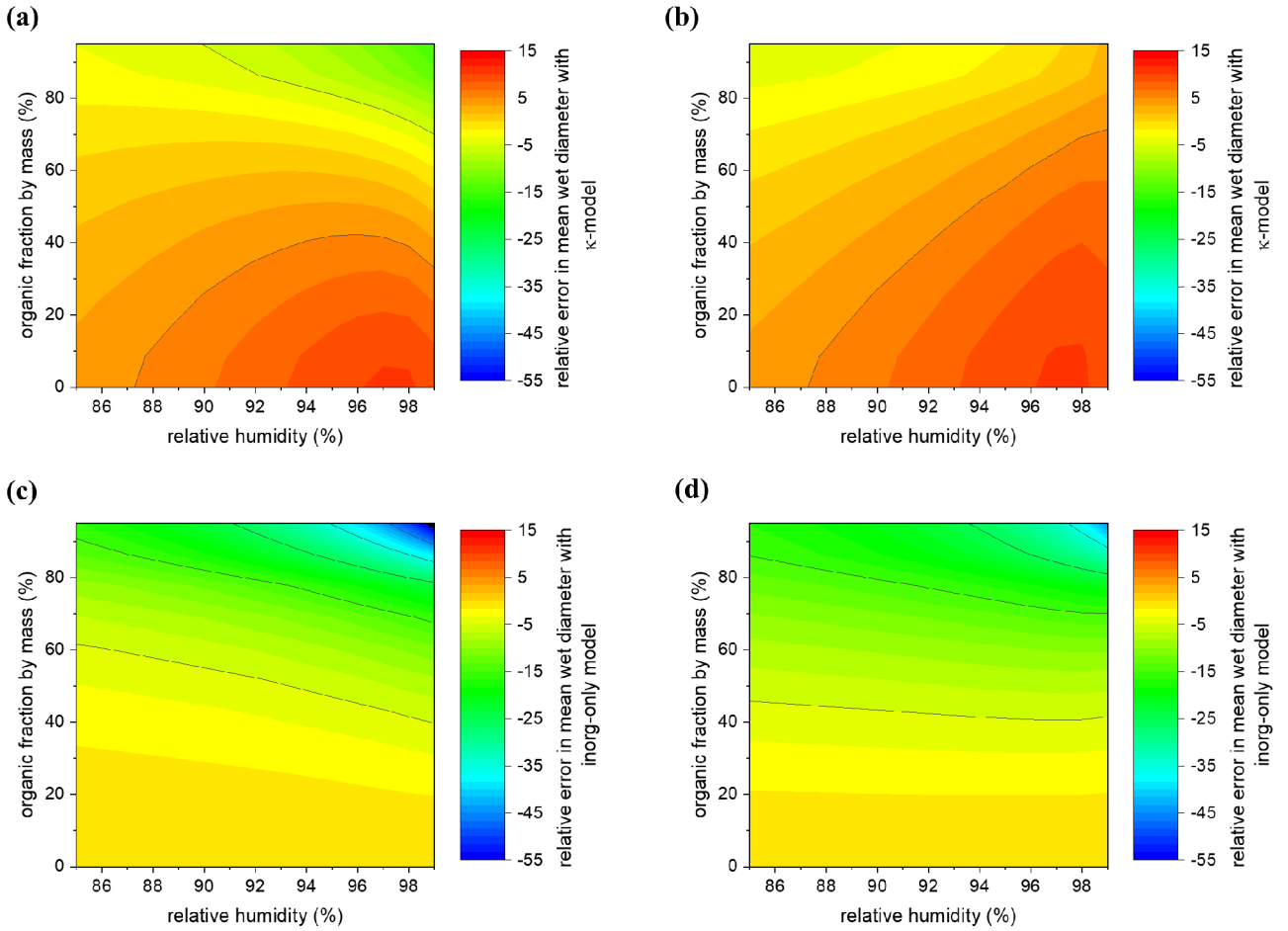

Figure 3. Contour plots of relative errors in mean D_{wet} with (a, b) κ-model (c, d) inorg-only model: (a, c) ammonium sulfate + glutaric acid; (b, d) ammonium sulfate + sucrose.

However, studies report κ values ranging from 0.01 to 0.3 depending on functional groups (Suda et al. 2012, 2014) and degree of oxidation (Kuang et al. 2020) suggesting potentially large uncertainties in water uptake and therefore aerosol climate forcing if a fixed value of 0.1 is used. Very recently, C. Zhang et al. (2021) reported κ measurements for D_{dry} less than 100 nm pure oxalic acid particles to be between 0.1 and 0.3 for RH between 80 and 99.5%.

2.4. Optical properties calculations

Lastly, to estimate the optical properties of the aerosol population of different chemical systems, Mie theory was used (Kerker 1969; Mishchenko and Travis 2008). Mie theory assumes a homogeneous spherical particle, where the size is the same order of the wavelength of light, to provide an analytical solution to Maxwell's equations based on aerosol composition, refractive index (volume mean of the refractive index of all components) and size distribution. The Mie theory is based on the interaction of an electromagnetic wave with a sphere. The BHMIE (homogeneous sphere) and BHCOAT (coated sphere) codes (Bohren and Huffman 1983) are used in MATLAB to calculate the scattering and absorption cross-sections for each particle, and the scattering and absorption coefficients and single scattering albedos for the whole particle distribution at wavelength, $\lambda = 550$ nm.

3. Sensitivity of water uptake to model assumptions and resulting errors in aerosol optical properties

Section 3.1 compares particle growth of organic/inorganic mixtures calculated using the Ad-iso model with the two simplified models mentioned in Sections 2.2 and 2.3, "inorg-only" and "κ," respectively. We present the results as a function of water-soluble organic mass fraction f, relative humidity RH, and particle dry diameter D_{dry}. In Section 3.2, we present how these errors propagate into the calculation of the aerosols' light scattering abilities. Section 3.3 includes calculations of light absorbing abilities for the case of black

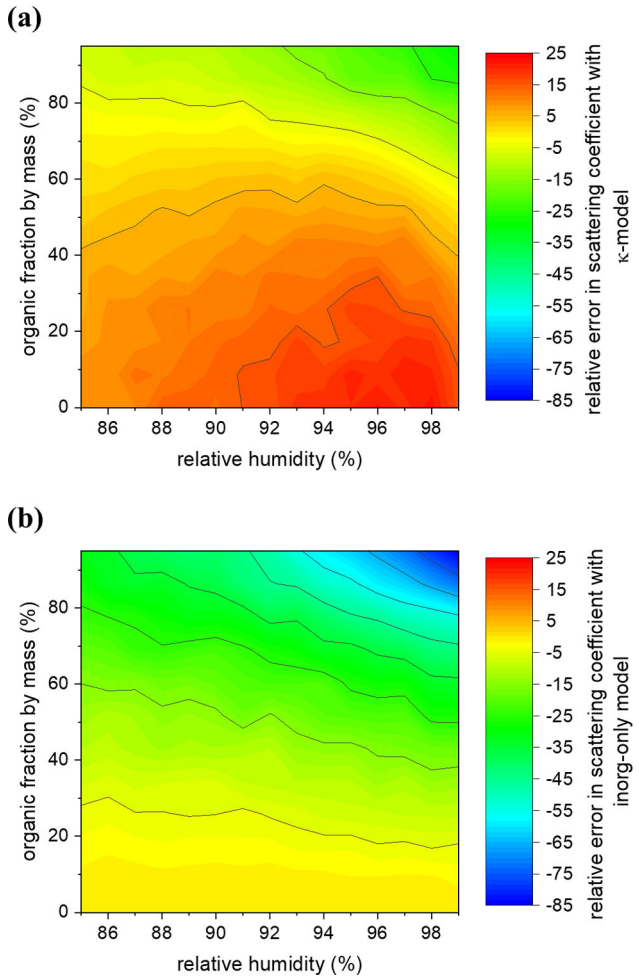

Figure 4. Relative errors in scattering coefficient of aerosol population for the whole distribution (ammonium sulfate + glutaric acid) with (a) κ-model and (b) inorg-only model.

carbon being present in the particle core. Note that f represents only the organic fraction that is water-soluble and does not include the black carbon for which $\kappa = 0$.

3.1. Particle growth in organic/inorganic mixtures

Figure 2a shows the hygroscopic growth factor, gf, as a function of dry particle size for the mixed particles (Ad-iso model in solid lines, κ-model in dashed lines, inorg-only model in dotted lines). Consistent with Figures 1c and d, the growth factor not only depended on the organic fraction, f, but also on the dry particle size, especially for dry diameters smaller than 300 nm due to the Kelvin effect. Since the κ-model used a fixed average value for the hygroscopicity parameter, it sometimes overpredicted [$f = 5$, 35, 55%] and other times underpredicted [$f = 95\%$] droplet growth depending on the mass fraction of organic species. In contrast, the inorg-only model underpredicted droplet growth in mixed particles, as it calculated the water uptake only by the inorganic components.

Figures 2b and c evaluate the relative error in droplet size as a function of relative humidity for particles with 90 nm dry diameter. We present the results separated by organic mass fraction range, with lower mass fractions ($f = 0$–55%) in Figure 2b, and higher mass fractions ($f = 65$–95%) in Figure 2c. The relative error was calculated by $\frac{D_x - D_{Ad-iso}}{D_{Ad-iso}}$, where D_x is the wet diameter calculated with the simplified models (κ or inorg-only) and D_{Ad-iso} is the wet diameter calculated with the reference model Ad-iso.

For the ammonium sulfate (AS) + glutaric acid (GA) system using the κ-model (dashed lines), the error varied from +15% to −10% as f increased from 0 to 95%. For lower organic fractions, the κ-model overpredicted droplet size, and for larger organic mass fractions, it underpredicted, with the lowest error occurring at *approximately* $f = 65\%$. The magnitude of these errors depended on the exact value of the fixed hygroscopicity parameter used in all the systems in this study for the κ-model. This informs us that a constant κ for each component may not be desirable for growth estimations in organic-inorganic mixed particles, depending on how accurately the growth needs to be determined. For the inorg-only case, droplet size was always underpredicted as expected, and the magnitude error increased from 0% to ∼ −55% as f increased from 0 to 95%.

Figure 3 shows contour plots for the relative errors in the geometric mean diameter of the wet size distribution (as shown in Figure 1a) over the RH range of 85 to 99% and the organic fraction range of 0 to 95% for the ternary systems AS + GA and AS + sucrose. The corresponding contour plots for the aerosol systems AS + SA and NaCl + sucrose are reported in the SI (Figure S4). Although the trends in the relative errors for the system AS + GA (Figures 3a and b) were comparable with the system AS + SA (Figures S2a and b), the contour plots for the other two systems containing sucrose exhibited very different patterns, specifically with the κ-model. This is due to the variation of κ with a_w for sucrose having an almost linear dependence compared to a U-shaped dependence for the other four compounds (Figure S2 – inorganics and Figure 1b – organics; the U-shaped trends agree with (Petters and Kreidenweis 2007) parameterization. Table S1 in the SI reports the mean wet diameters after water uptake with varying organic fractions and relative humidities. The table also compares mean diameters calculated from all the three models in this study.

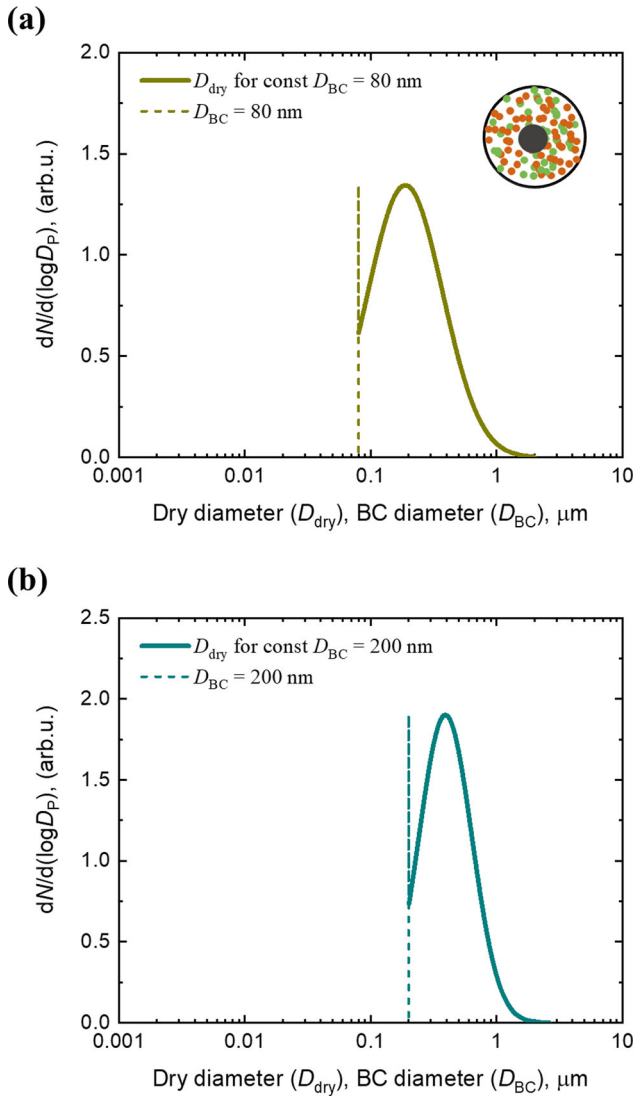

Figure 5. Dry size distribution of water-soluble internally mixed particles containing black carbon core (a) D_{BC} = 80 nm (b) D_{BC} = 200 nm. Inset: green spheres – organic molecules, orange spheres – inorganic molecules, black sphere – aggregates of black carbon assumed as a sphere in the core.

3.2. Optical properties of the aerosol population containing non-absorbing organic/inorganic mixtures

We will next quantify the error in aerosol scattering that follows from errors in water uptake predictions. For water-soluble species of different compositions, the size distributions of particles at different relative humidities are required, which have been computed in Section 3.1. The refractive indices of the species in this study and water were volume-averaged with respect to the compositions. The single-component real refractive indices at wavelength, $\lambda = 550$ nm were taken from (Wang and Rood 2008) (AS: 1.53, GA: 1.42, SA: 1.45, water: 1.33). The imaginary refractive indices for the water-soluble aerosol species were assumed zero as they are typically less than 0.01 (Moise, Flores, and Rudich 2015; Laskin, Laskin, and Nizkorodov 2015). The refractive index used for NaCl is 1.55-0i (Pinnick and Auvermann 1979), and for sucrose is 1.5-0i (Hess, Koepke, and Schult 1998). The aerosol optical properties were then computed using Mie theory assuming spherical and homogeneous particles.

The light scattering efficiencies (Q_{sca}, dimensionless) were calculated using the code "BHMIE" (Bohren and Huffman 1983), having inputs – wavelength of incoming light, refractive index of each particle, and size of the particle. The scattering cross-sections ($\sigma_{sca} = (\pi/4)\ Q_{sca}\ D_{wet}^2$) were then calculated for each particle to determine the volume scattering coefficient, β_{sca}, by summing σ_{sca} over all particles per unit volume of air for the entire aerosol population.

Figure 4 shows the contour plots of the relative errors in volume scattering coefficient with both the simplified models calculated in the same way as particle size errors in the previous section. The contours have similar patterns as in Figure 3, with the scattering coefficient errors ranging from around +25% to −30% for the κ-model, and from 0% to −85% for the inorg-only model for the AS + GA system. The range of errors for the other three systems were of similar magnitude. The large errors imply that the scattering and hence the cooling effect of aerosols is sensitive to the differences in water uptake, and that the cooling determined by particles with high organic fractions may be highly underpredicted by the inorg-only model.

The absolute scattering coefficients calculated using Ad-iso for AS + GA system of particles are shown in Figure S5 (dash-dot line). The backscattering coefficients with respect to RH are also shown in Figure S5 (solid line) for $f = 0$, 55 and 95%. The symbols in Figure S5 represent the percentage of the scattered light that is scattered back to space (values on the right axis). The percentage backscatter is mostly between 30 and 40%, having no particular trend with f or RH.

3.3. Optical properties of the aerosol population containing absorbing black carbon cores and non-absorbing mixed organic/inorganic coatings

So far, the particle growth studies presented here were limited to non-absorbing aerosol species. For studying the absorption properties, we considered black carbon in the core of the particles with dry size distribution as shown in Figure 5. To investigate the effect of hydrophobic core size on light absorption, the core sizes (D_{BC}) studied were 80 nm and 200 nm (Bond, Habib, and Bergstrom 2006; Bond et al. 2013; Fierce et al.

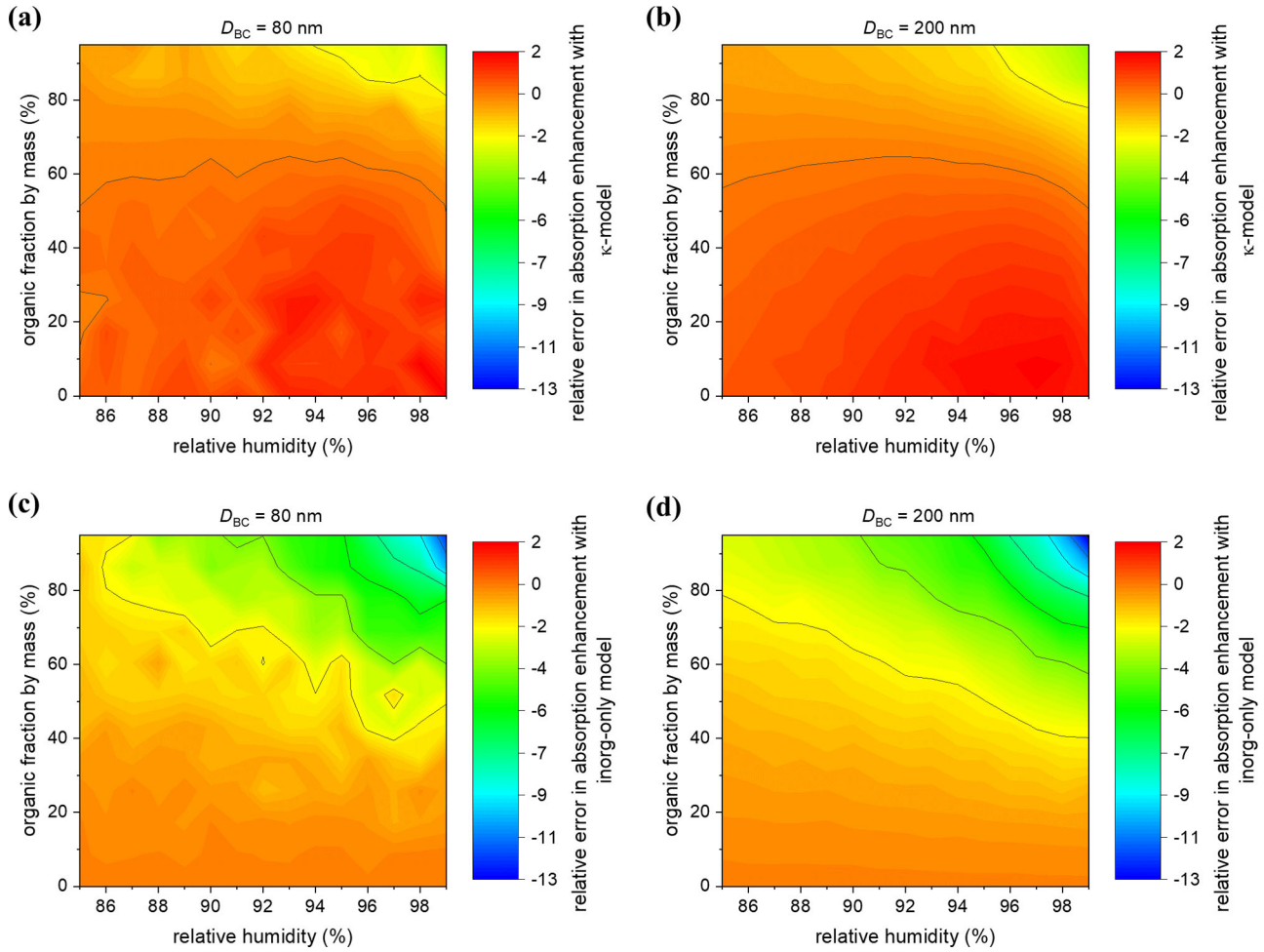

Figure 6. Contour plots (ammonium sulfate + glutaric acid) for relative errors in absorption enhancement of BC containing aerosol distribution with (a, b) the κ-model – D_{BC} = 80 nm, 200 nm and (c, d) the inorg-only model – D_{BC} = 80 nm, 200 nm.

2020; Schwarz et al. 2006). For each aerosol distribution, the core size was fixed. Only the coating thickness varied and increased further with water uptake.

The code "BHCOAT" (Bohren and Huffman 1983) was used to calculate the scattering and absorption properties for particles assuming a concentric-sphere morphology (core-shell) of the BC core (light absorbing material) and internally mixed water-soluble species coating/shell (non-absorbing material). The refractive index used for black carbon in the calculations was 1.95–0.79i (Bond and Bergstrom 2006) at wavelength, $\lambda = 550$ nm. The lensing effect caused light absorption of BC to be enhanced by the non-absorbing coating, given by Equation (4).

$$\text{Absorption enhancement} = \frac{\text{absorption cross section of the whole droplet}}{\text{absorption cross section of the bare BC}} \quad (4)$$

A normalized absorption cross-section to the mass of the black carbon (MAC_{BC}) was defined by Bond and coworkers (Bond and Bergstrom 2006; Bond, Habib, and Bergstrom 2006; Bond et al. 2013) as

$$MAC_{BC} = \frac{\text{absorption cross section of BC containing particles}(m^2)}{\text{mass concentration of the BC core (g)}} \quad (5)$$

For the aerosol distribution in this study, the MAC_{BC} calculated using the Ad-iso model varied between 5.9 and 11.5 m^2/g for core diameters between 80 nm and 200 nm, which is in the range of reported MAC_{BC} in the literature (Bond and Bergstrom 2006; Koch et al. 2009; Schuster et al. 2005).

Errors in calculated water uptake influenced the calculated absorption enhancement through two distinct effects that tended to compensate each other. An underestimation of water uptake resulted in an underestimated coating thickness which, on the one hand, reduced the lensing effect. On the other hand, the volume-averaged refractive index of this coating was overestimated. The overall outcome of light absorption enhancement errors caused by errors in water uptake calculations is shown in Figure 6. Although

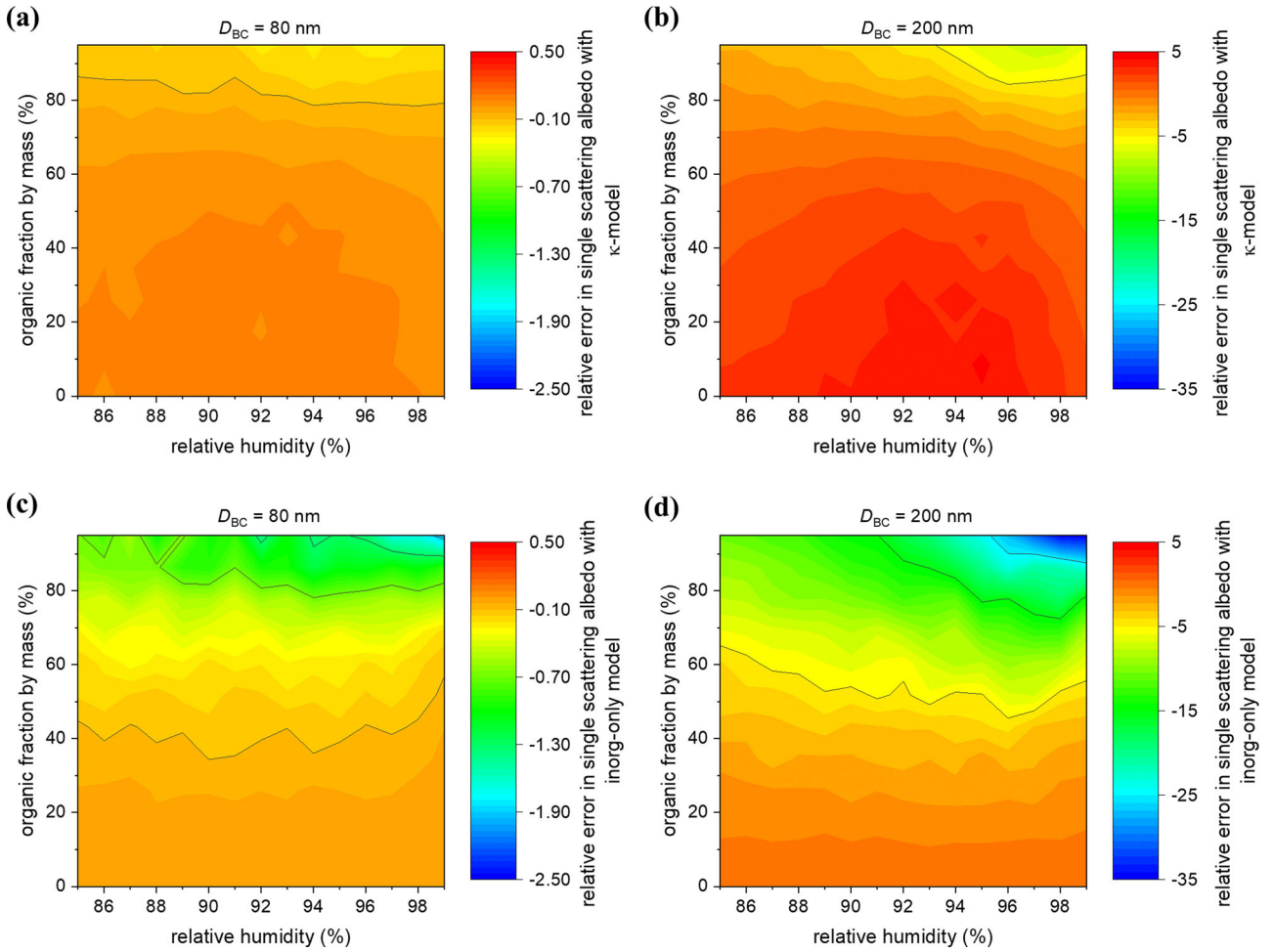

Figure 7. Contour plots (ammonium sulfate + glutaric acid) for relative errors in single scattering albedo of BC containing aerosol distribution with (a, b) κ-model – D_{BC} = 80 nm, 200 nm and (c, d) inorg-only model – D_{BC} = 80 nm, 200 nm.

the error patterns were similar to the ones for the water uptake and scattering, the magnitude of errors were lower due to the two compensating effects (demonstrated in Figures S6 and S7). The absorption enhancement errors ranged from ~+2% to ~–3% for the κ-model, and from ~0% to ~–13% for the inorg-only model for the AS + GA system. The range of errors for the other three systems were approximately the same.

Contour plot of errors in single scattering albedo (ω), the ratio of scattering cross section and extinction cross section, of both the models are shown in Figure 7. The absolute values (calculated by Ad-iso model) contour plots of ω are reported in Figure S8. It is important to note that ω was between 0.983 and 0.998 for particles with an 80 nm BC core, and as low as 0.57 with a 200 nm BC core. The ω values estimated by the simplified models were comparable resulting in low errors (up to 2.5%) for the smaller core as shown in Figures 7a and c. However, the errors for particles with a 200 nm core were higher (up to 35%) as shown in Figures 7b and d, which is explained in more detail in the SI (Figure S9).

3.4. Direct aerosol radiative forcing: Uncertainty and sensitivity

In this section, the effect of single scattering albedo error on direct aerosol radiative forcing (DARF) uncertainty is discussed. DARF is highly sensitive to errors in single scattering albedo and the sensitivity increases for lower values of ω (McComiskey et al. 2008; Loeb and Su 2010; Thorsen et al. 2020). McComiskey et al. (2008) suggested that DARF accuracy can be increased by a small decrease in the ω uncertainty because the sensitivity of DARF to ω, $S_\omega = \frac{\partial F}{\partial \omega}$, was found to be most significant compared to other parameters such as aerosol optical depth, asymmetry parameter and surface albedo. They reported S_ω to be ~−10 W/m^2 for ω = 0.97 and −30 to −70 W/m^2 for ω = 0.95, which is in line with other studies (Thorsen et al. 2020; Loeb and Su 2010).

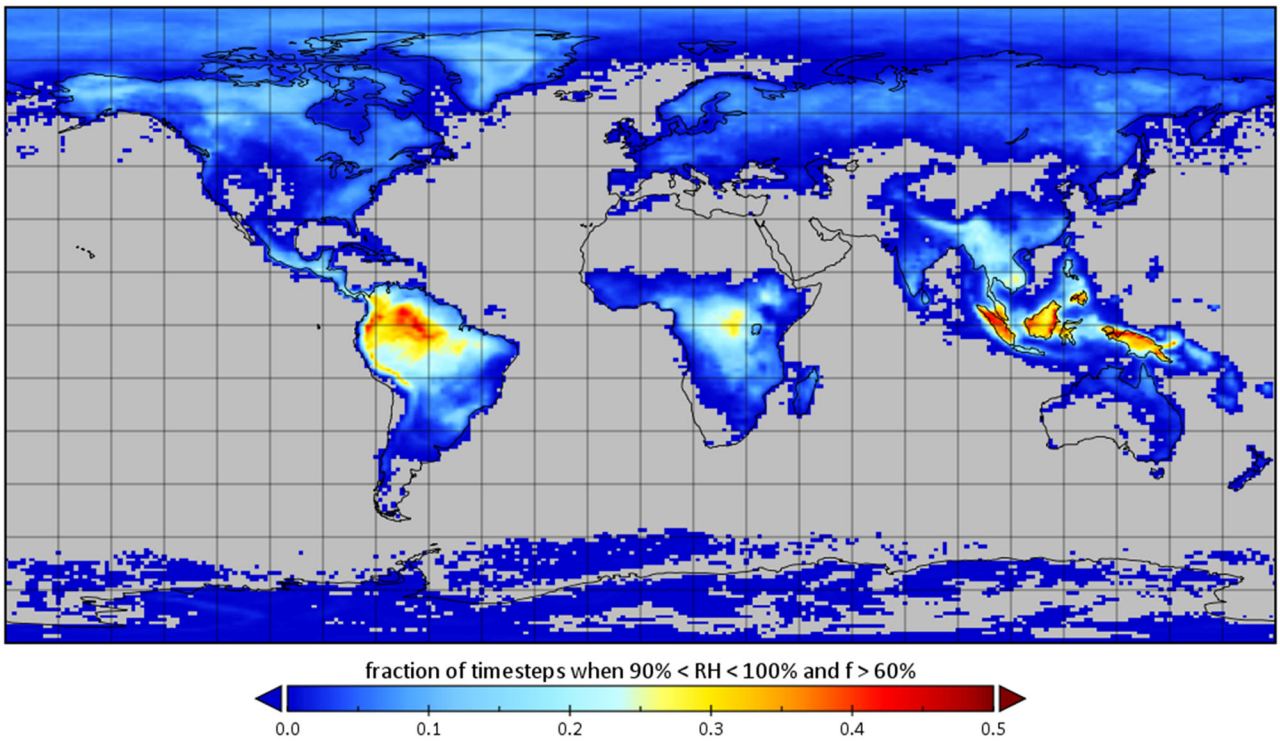

Figure 8. Contour plot in the real atmosphere on a global scale for the year 2011 showing spatial variability where high values of RH coincide with high values of f (90% $<$ RH $<$ 100% and $f >$ 60%). The data is from the Community Earth System Model (CESM version 2.1.0) component Community Atmospheric Model (CAM6) (Bogenschutz et al. 2018) simulation resolved for one year every 3 h on a 0.9° latitude $\times$ 1.25° longitude grid (Zheng et al. 2021).

In this article, we report an underestimation of ω by the simplified models by 5% or more for ω between 0.57 and 0.91, and by up to 2% for ω higher than 0.98, both at high organic fractions and high relative humidities. For the current study, if we select the 80 nm BC core size with our defined size distribution, the highest DARF uncertainty near the surface would be 0.2 W/m^2 given a $S_\omega = -10$ W/m^2 sensitivity. And if we select the 200 nm core, the sensitivity could be much higher, e.g., $S_\omega = -50$ W/m^2 and therefore, the DARF uncertainty for a $\Delta\omega$ of -5% with a baseline ω of 0.75 would result in an error of radiative forcing on the order of 1.75 W/m^2.

Figure 8 quantifies where conditions occur when high values of f coincide with high values of RH thereby leading to largest errors in DARF. We used 3-h global modeling outputs from the CESM (Community Earth System Model) for the year 2011. The outputs were from a typical historical simulation of the Community Atmospheric Model (CAM6), which uses the 4-mode version of Modal Aerosol Module (MAM4) (Liu et al. 2016). MAM4 predicts the six aerosol species (BC, dust, sea salt, primary organic matter (POM), secondary organic aerosol (SOA), and sulfate) across four lognormal modes (Aitken, accumulation, coarse, and primary carbon modes). Maps of the six aerosol species concentrations are shown in Figure S10 of the SI. We counted the relative frequency of occurrence when f was larger than 60% and at the same time RH was between 90% and 100%. For example, a value of 0.5 on the map in Figure 8 means that this criterion was fulfilled for 50% of the output timesteps. The map shows that the highest frequencies occurred over the Amazon region, central Africa, and Indonesia. For the continental US, a frequency of up to 20% was indicated that could result in high DARF errors. For reference, in the areas where f exceeded 60% and RH was between 90% and 100% for at least 25% of the output timesteps, the average mass mixing ratios of SOA and POM were 7.1 μg/kg (SOA) and 2.7 μg/kg (POM), respectively.

4. Summary and conclusions

This study investigated the water uptake of mixed organic/inorganic aerosols and quantified the error in growth factor and optical properties that was incurred by simplifying assumptions commonly made in current chemical transport models. In particular, we explored the errors when (1) assuming that organic species did not contribute to water uptake at all, and (2) when the water uptake of organic/inorganic

mixtures was represented by constant hygroscopicity parameters for each constituent. We used the accurate lattice-based adsorption isotherm model (Ad-iso) as a benchmark for calculating water uptake of mixtures containing ammonium sulfate or sodium chloride as inorganic species, and glutaric acid, succinic acid or sucrose as organic species, with and without a core of absorbing black carbon, under conditions of relative humidity larger than 85%. We did not consider feedback effects on gas-particle partitioning which may be important (Pye et al. 2017). We limited this investigation to high RH conditions because we used the surface tension of water instead of the solution mixture in the Köhler equation.

For particles with an organic mass fraction of 50%, completely neglecting the water uptake by organic components led to errors up to 77% in growth factor, up to 23% in volume scattering coefficient, up to 2.5% in absorption enhancement and up to 3.5% in single scattering albedo. Larger errors occurred for increasing organic mass fractions and were up to 35% for single scattering albedo for an organic mass fraction of 95%.

Approximating the organic water uptake with a constant hygroscopicity parameter κ (here κ was set to 0.1), the errors were smallest for organic mass fractions between 45 and 65%, and remained within 3% for the growth factor, 4% for the volume scattering coefficient, 0.5% for the absorption enhancement and 0.6% for the single scattering albedo. For organic mass fractions smaller than 45% or larger than 65%, the errors increased to 6% for the single scattering albedo.

Single scattering albedo is of particular importance for calculating the direct aerosol radiative forcing (McComiskey et al. 2008; Loeb and Su 2010), and the sensitivity of radiative forcing depends on the value of ω. Errors in ω of a few percent matter for predicting DARF. Completely neglecting aerosol water uptake by organics introduced errors of a magnitude that is relevant for direct aerosol forcing calculations. Approximating aerosol water uptake by organics by a constant κ value led to lower errors, which may be acceptable for the range of organic mass fractions between 45 and 65%. For organic mass fractions outside this range, the errors are still large enough to matter for DARF calculations. To estimate to what extent different regions are prone to experiencing these errors, we used output from CESM and constructed a frequency distribution of occurrences when f is larger than 60% and at the same time RH is larger than 90%. These conditions are fulfilled for a frequency of up to 50% over the Amazon region, central Africa, and Indonesia, and up to 20% over the continental US.

Code availability

The code is available on github – https://github.com/lucy-nandy/AerosolWaterUptake

The main code calls an optimization function to calculate the water activity and another to calculate the molality of the solution mixture. The second part of the code calls the BHMIE and BHCOAT functions. For 10000 computational particles in a distribution, at a particular relative humidity and organic fraction, the entire code run takes approximately 900 s on a Intel Core i7 processor.

Funding

NR and YY acknowledge funding from grant NSF AGS 1941110.

ORCID

Lucy Nandy http://orcid.org/0000-0001-7647-9837
Yu Yao http://orcid.org/0000-0001-7690-0353
Zhonghua Zheng http://orcid.org/0000-0002-0642-650X
Nicole Riemer http://orcid.org/0000-0002-3220-3457

References

Adachi, K., and P. R. Buseck. 2008. Internally mixed soot, sulfates, and organic matter in aerosol particles from Mexico City. *Atmos. Chem. Phys.* 8 (21):6469–81. doi:10.5194/acp-8-6469-2008.

Appel, K. W., G. A. Pouliot, H. Simon, G. Sarwar, H. O. T. Pye, S. L. Napelenok, F. Akhtar, and S. J. Roselle. 2013. Evaluation of dust and trace metal estimates from the community multiscale air quality (CMAQ) model version 5.0. *Geosci. Model Dev.* 6 (4):883–99. doi:10.5194/gmd-6-883-2013.

Asa-Awuku, A., A. Nenes, S. Gao, R. C. Flagan, and J. H. Seinfeld. 2010. Water-soluble SOA from alkene ozonolysis: Composition and droplet activation kinetics inferences from analysis of CCN activity. *Atmos. Chem. Phys.* 10 (4):1585–97. doi:10.5194/acp-10-1585-2010.

Bogenschutz, P. A., A. Gettelman, C. Hannay, V. E. Larson, R. B. Neale, C. Craig, and C. C. Chen. 2018. The path to CAM6: Coupled simulations with CAM5.4 and CAM5.5. *Geosci. Model Dev.* 11 (1):235–55. doi:10.5194/gmd-11-235-2018.

Bohren, C. F., and D. R. Huffman. 1983. *Absorption and scattering of light by small particles*. New York: John Wiley & Sons, Inc.

Bond, T. C., and R. W. Bergstrom. 2006. Light absorption by carbonaceous particles: An investigative review. *Aerosol Sci. Technol.* 40 (1):27–67. doi:10.1080/02786820500421521.

Bond, T. C., S. J. Doherty, D. W. Fahey, P. M. Forster, T. Berntsen, B. J. DeAngelo, M. G. Flanner, S. Ghan, B.

Kärcher, D. Koch, et al. 2013. Bounding the role of black carbon in the climate system: A scientific assessment. *J. Geophys. Res. Atmos.* 118 (11):5380–552. doi:10.1002/jgrd.50171.

Bond, T. C., G. Habib, and R. W. Bergstrom. 2006. Limitations in the enhancement of visible light absorption due to mixing state. *J. Geophys. Res.* 111 (D20):1–13. doi:10.1029/2006JD007315.

Burgos, M. A., E. Andrews, G. Titos, L. Alados-Arboledas, U. Baltensperger, D. Day, A. Jefferson, N. Kalivitis, N. Mihalopoulos, J. Sherman, et al. 2019. A global view on the effect of water uptake on aerosol particle light scattering. *Sci. Data.* 6 (1):157–19. doi:10.1038/s41597-019-0158-7.

Cai, C., R. E. H. Miles, M. I. Cotterell, A. Marsh, G. Rovelli, A. M. J. Rickards, Y. H. Zhang, and J. P. Reid. 2016. Comparison of methods for predicting the compositional dependence of the density and refractive index of organic-aqueous aerosols. *J. Phys. Chem. A.* 120 (33):6604–17. doi:10.1021/acs.jpca.6b05986.

Cai, C., D. J. Stewart, J. P. Reid, Y.-h. Zhang, P. Ohm, C. S. Dutcher, and S. L. Clegg. 2015. Organic component vapor pressures and hygroscopicities of aqueous aerosol measured by optical tweezers. *J. Phys. Chem. A.* 119 (4):704–18. doi:10.1021/jp510525r.

Cappa, C. D., T. B. Onasch, P. Massoli, D. R. Worsnop, T. S. Bates, E. S. Cross, P. Davidovits, J. Hakala, K. L. Hayden, B. T. Jobson, et al. 2012. Radiative absorption enhancements due to the mixing state of atmospheric black carbon. *Science* 337 (6098):1078–81. doi:10.1126/science.1223447.

Craig, R. L., L. Nandy, J. L. Axson, C. S. Dutcher, and A. P. Ault. 2017. Spectroscopic determination of aerosol PH from acid-base equilibria in inorganic, organic, and mixed systems. *J. Phys. Chem. A.* 121 (30):5690–9. doi:10.1021/acs.jpca.7b05261.

Craig, R. L., P. K. Peterson, L. Nandy, Z. Lei, M. A. Hossain, S. Camarena, R. A. Dodson, R. D. Cook, C. S. Dutcher, and A. P. Ault. 2018. Direct determination of aerosol PH: Size-resolved measurements of submicrometer and supermicrometer aqueous particles. *Anal. Chem.* 90 (19):11232–9. doi:10.1021/acs.analchem.8b00586.

Dutcher, C. S., X. Ge, A. S. Wexler, and S. L. Clegg. 2011. Statistical mechanics of multilayer sorption: Extension of the Brunauer–Emmett–Teller (BET) and Guggenheim–Anderson–de Boer (GAB) adsorption isotherms. *J. Phys. Chem. C.* 115 (33):16474–87. doi:10.1021/jp203879d.

Dutcher, C. S., X. Ge, A. S. Wexler, and S. L. Clegg. 2012. Statistical mechanics of multilayer sorption: 2. Systems containing multiple solutes. *J. Phys. Chem. C.* 116 (2):1850–64. doi:10.1021/jp2084154.

Dutcher, C. S., X. Ge, A. S. Wexler, and S. L. Clegg. 2013. An isotherm-based thermodynamic model of multicomponent aqueous solutions, applicable over the entire concentration range. *J. Phys. Chem. A.* 117 (15):3198–213. doi:10.1021/jp310860p.

Engelhart, G. J., A. Asa-Awuku, A. Nenes, and S. N. Pandis. 2008. CCN activity and droplet growth kinetics of fresh and aged monoterpene secondary organic aerosol. *Atmos. Chem. Phys.* 8 (14):3937–49. doi:10.5194/acp-8-3937-2008.

Estillore, A. D., H. S. Morris, V. W. Or, H. D. Lee, M. R. Alves, M. A. Marciano, O. Laskina, Z. Qin, A. V. Tivanski, and V. H. Grassian. 2017. Linking hygroscopicity and the surface microstructure of model inorganic salts, simple and complex carbohydrates, and authentic sea spray aerosol particles. *Phys. Chem. Chem. Phys.* 19 (31):21101–11. doi:10.1039/c7cp04051b.

Fierce, L., T. C. Bond, S. E. Bauer, F. Mena, and N. Riemer. 2016. Black carbon absorption at the global scale is affected by particle-scale diversity in composition. *Nat. Commun.* 7:12361–8. doi:10.1038/ncomms12361.

Fierce, L., T. B. Onasch, C. D. Cappa, C. Mazzoleni, S. China, J. Bhandari, P. Davidovits, D. A. Fischer, T. Helgestad, A. T. Lambe, et al. 2020. Radiative absorption enhancements by black carbon controlled by particle-to-particle heterogeneity in composition. *Proc. Natl. Acad. Sci. USA.* 117 (10):5196–203. doi:10.1073/pnas.1919723117.

Fountoukis, C., and A. Nenes. 2007. ISORROPIA II: A computationally efficient thermodynamic equilibrium model for K^+–Ca^{2+}–Mg^{2+}–NH_4^+–Na^+–SO_4^{2-}–NO_3^-–Cl^-–H_2O aerosols. *Atmos. Chem. Phys.* 7 (17):4639–59. . doi:10.5194/acp-7-4639-2007.

Fredenslund, A., R. L. Jones, and J. M. Prausnitz. 1975. Group-contribution estimation of activity coefficients in nonideal liquid mixtures. *AIChE J.* 21 (6):1086–99. doi:10.1002/aic.690210607.

Fuzzi, S., U. Baltensperger, K. Carslaw, S. Decesari, H. Denier van der Gon, M. C. Facchini, D. Fowler, I. Koren, B. Langford, U. Lohmann, et al. 2015. Particulate matter, air quality and climate: Lessons learned and future needs. *Atmos. Chem. Phys.* 15 (14):8217–99. doi:10.5194/acp-15-8217-2015.

Gorkowski, K., T. C. Preston, and A. Zuend. 2019. Relative-humidity-dependent organic aerosol thermodynamics via an efficient reduced-complexity model. *Atmos. Chem. Phys.* 19 (21):13383–407. doi:10.5194/acp-19-13383-2019.

Griffin, R. J., K. Nguyen, D. Dabdub, and J. H. Seinfeld. 2003. A coupled hydrophobic-hydrophilic model for predicting secondary organic aerosol formation. *J. Atmos. Chem.* 44 (2):171–90. doi:10.1023/A:1022436813699.

Heal, M. R., P. Kumar, and R. M. Harrison. 2012. Particles, air quality, policy and health. *Chem. Soc. Rev.* 41 (19):6606–30. doi:10.1039/c2cs35076a.

Hess, M., P. Koepke, and I. Schult. 1998. Optical properties of aerosols and clouds: The software package OPAC. *Bull. Amer. Meteor. Soc.* 79 (5):831–44. doi:10.1175/1520-0477(1998)079<0831:OPOAAC>2.0.CO;2.

Hodas, N., A. Zuend, W. Mui, R. C. Flagan, and J. H. Seinfeld. 2015. Influence of particle-phase state on the hygroscopic behavior of mixed organic-inorganic aerosols. *Atmos. Chem. Phys.* 15 (9):5027–45. doi:10.5194/acp-15-5027-2015.

Jacobson, M. Z. 1999. Studying the effects of calcium and magnesium on size-distributed nitrate and ammonium with EQUISOLV II. *Atmos. Environ.* 33 (22):3635–49. doi:10.1016/S1352-2310(99)00105-3.

Jacobson, M. Z., A. Tabazadeh, and R. P. Turco. 1996. Simulating equilibrium within aerosols and nonequilibrium between gases and aerosols. *J. Geophys. Res.* 101 (D4):9079–91. doi:10.1029/96JD00348.

Jefferson, A., D. Hageman, H. Morrow, F. Mei, and T. Watson. 2017. Seven years of aerosol scattering hygroscopic growth measurements from SGP: Factors influencing water uptake. *J. Geophys. Res. Atmos.* 122 (17): 9451–66. doi:10.1002/2017JD026804.

Jing, B., S. Tong, Q. Liu, K. Li, W. Wang, Y. Zhang, and M. Ge. 2016. Hygroscopic behavior of multicomponent organic aerosols and their internal mixtures with ammonium sulfate. *Atmos. Chem. Phys.* 16 (6):4101–18. doi:10.5194/acp-16-4101-2016.

Kawamura, K., and K. Ikushima. 1993. Seasonal changes in the distribution of dicarboxylic acids in the urban atmosphere. *Environ. Sci. Technol.* 27 (10):2227–35. doi:10.1021/es00047a033.

Kerker, M. 1969. *The scattering of light and other electromagnetic radiation*. New York : Academic Press.

Kim, Y. P., and J. H. Seinfeld. 1995. Atmospheric gas–aerosol equilibrium: III. Thermodynamics of crustal elements Ca^{2+}, K^{+}, and Mg^{2+}. *Aerosol Sci. Technol.* 22 (1):93–110. doi:10.1080/02786829408959730.

Knox, A., G. J. Evans, J. R. Brook, X. Yao, C. H. Jeong, K. J. Godri, K. Sabaliauskas, and J. G. Slowik. 2009. Mass absorption cross-section of ambient black carbon aerosol in relation to chemical age. *Aerosol Sci. Technol.* 43 (6): 522–32. doi:10.1080/02786820902777207.

Koch, D., M. Schulz, S. Kinne, C. McNaughton, J. R. Spackman, Y. Balkanski, S. Bauer, T. Berntsen, T. C. Bond, O. Boucher, et al. 2009. Evaluation of black carbon estimations in global aerosol models. *Atmos. Chem. Phys.* 9 (22):9001–26. doi:10.5194/acp-9-9001-2009.

Kou, L. 1996. *Black carbon: Atmospheric measurements and radiative effect*. Canada: Dalhousie University.

Kuang, Y., W. Xu, J. Tao, N. Ma, C. Zhao, and M. Shao. 2020. A review on laboratory studies and field measurements of atmospheric organic aerosol hygroscopicity and its parameterization based on oxidation levels. *Curr. Pollution Rep.* 6 (4):410–24. doi:10.1007/s40726-020-00164-2.

Laliberte, M., and W. E. Cooper. 2004. Model for calculating the density of aqueous electrolyte solutions. *J. Chem. Eng. Data* 49 (5):1141–51. doi:10.1021/je0498659.

Laskin, A., J. Laskin, and S. A. Nizkorodov. 2015. Chemistry of atmospheric brown carbon. *Chem. Rev.* 115 (10):4335–82. doi:10.1021/cr5006167.

Liu, X., P. Ma, H. Wang, S. Tilmes, B. Singh, R. C. Easter, S. J. Ghan, and P. J. Rasch. 2016. Description and evaluation of a new four-mode version of the modal aerosol module (MAM4) within version 5.3 of the community atmosphere model. *Geosci. Model Dev.* 9 (2):505–22. doi:10.5194/gmd-9-505-2016.

Loeb, N. G., and W. Su. 2010. Direct aerosol radiative forcing uncertainty based on a radiative perturbation analysis. *Journal of Climate* 23 (19):5288–93. doi:10.1175/2010JCLI3543.1.

Marsh, A., R. E. H. Miles, G. Rovelli, A. G. Cowling, L. Nandy, C. S. Dutcher, and J. P. Reid. 2017. Influence of organic compound functionality on aerosol hygroscopicity: Dicarboxylic acids, alkyl-substituents, sugars and amino acids. *Atmos. Chem. Phys.* 17 (9):5583–99. doi:10.5194/acp-17-5583-2017.

Marshall, F. H., T. Berkemeier, M. Shiraiwa, L. Nandy, P. B. Ohm, C. S. Dutcher, and J. P. Reid. 2018. Influence of particle viscosity on mass transfer and heterogeneous ozonolysis kinetics in aqueous-sucrose-maleic acid aerosol. *Phys. Chem. Chem. Phys.* 20 (22):15560–73. doi:10.1039/c8cp01666f.

Marshall, F. H., R. E. H. Miles, Y.-C. Song, P. B. Ohm, R. M. Power, J. P. Reid, and C. S. Dutcher. 2016. Diffusion and reactivity in ultraviscous aerosol and the correlation with particle viscosity. *Chem. Sci.* 7 (2): 1298–308. doi:10.1039/c5sc03223g.

McComiskey, A., S. E. Schwartz, B. Schmid, H. Guan, E. R. Lewis, P. Ricchiazzi, and J. A. Ogren. 2008. Direct aerosol forcing: Calculation from observables and sensitivities to inputs. *J. Geophys. Res.* 113 (D9):1–16. doi:10.1029/2007JD009170.

McFiggans, G., P. Artaxo, U. Baltensperger, H. Coe, M. C. Facchini, G. Feingold, S. Fuzzi, M. Gysel, A. Laaksonen, U. Lohmann, et al. 2006. The effect of physical and chemical aerosol properties on warm cloud droplet activation. *Atmos. Chem. Phys.* 6 (9):2593–649. doi:10.5194/acp-6-2593-2006.

Meng, Z., J. H. Seinfeld, P. Saxena, and Y. P. Kim. 1995. Atmospheric gas-aerosol equilibrium: IV. Thermodynamics of carbonates. *Aerosol Sci. Technol.* 23 (2):131–54. doi:10.1080/02786829508965300.

Metzger, S., F. Dentener, M. Krol, A. Jeuken, and J. Lelieveld. 2002. Gas/aerosol partitioning 2. Global modeling results. *J. Geophys. Res.* 107 (D16):1–23. doi:10.1029/2001JD001103.

Metzger, S., F. Dentener, S. Pandis, and J. Lelieveld. 2002. Gas/aerosol partitioning: 1. A computationally efficient model. *J. Geophys. Res.* 107 (D16):1–24. doi:10.1029/2001JD001102.

Mishchenko, M. I., and L. D. Travis. 2008. Gustav Mie and the evolving subject of light scattering by particles. *Bull. Am. Meteorol. Soc.* 89 (12):1853–61. doi:10.1063/1.3116928.

Moise, T., J. M. Flores, and Y. Rudich. 2015. Optical properties of secondary organic aerosols and their changes by chemical processes. *Chem. Rev.* 115 (10):4400–39. doi:10.1021/cr5005259.

Moosmüller, H., R. K. Chakrabarty, and W. P. Arnott. 2009. Aerosol light absorption and its measurement: A review. *J. Quant. Spectrosc. Radiat. Transf.* 110 (11): 844–78. doi:10.1016/j.jqsrt.2009.02.035.

Naik, V., L. W. Horowitz, A. M. Fiore, P. Ginoux, J. Mao, A. M. Aghedo, and H. Levy. 2013. Impact of preindustrial to present-day changes in short-lived pollutant emissions on atmospheric composition and climate forcing. *J. Geophys. Res. Atmos.* 118 (14):8086–110. doi:10.1002/jgrd.50608.

Nandy, L., and C. S. Dutcher. 2017. Isotherm-based thermodynamic model for solute activities of asymmetric electrolyte aqueous solutions. *J. Phys. Chem. A.* 121 (37): 6957–65. doi:10.1021/acs.jpca.7b03649.

Nandy, L., P. B. Ohm, and C. S. Dutcher. 2016. Isotherm-based thermodynamic models for solute activities of organic acids with consideration of partial dissociation. *J. Phys. Chem. A.* 120 (24):4147–54. doi:10.1021/acs.jpca.6b01904.

O'Brien, R. E., B. Wang, S. T. Kelly, N. Lundt, Y. You, A. K. Bertram, S. R. Leone, A. Laskin, and M. K. Gilles. 2015. Liquid-liquid phase separation in aerosol particles:

Imaging at the nanometer scale. *Environ. Sci. Technol.* 49 (8):4995–5002. doi:10.1021/acs.est.5b00062.

Ohm, P. B., C. Asato, A. S. Wexler, and C. S. Dutcher. 2015. Isotherm-based thermodynamic model for electrolyte and nonelectrolyte solutions incorporating long- and short-range electrostatic interactions. *J. Phys. Chem. A.* 119 (13):3244–52. doi:10.1021/jp512646k.

Peng, C., M. N. Chan, and C. K. Chan. 2001. The hygroscopic properties of dicarboxylic and multifunctional acids: Measurements and UNIFAC predictions. *Environ. Sci. Technol.* 35 (22):4495–501. doi:10.1021/es0107531.

Peng, C., B. Jing, Y.-C. Guo, Y.-H. Zhang, and M.-F. Ge. 2016. Hygroscopic behavior of multicomponent aerosols involving NaCl and dicarboxylic acids. *J. Phys. Chem. A.* 120 (7):1029–38. doi:10.1021/acs.jpca.5b09373.

Petters, M. D., and S. M. Kreidenweis. 2007. A single parameter representation of hygroscopic growth and cloud condensation nucleus activity. *Atmos. Chem. Phys.* 7 (8): 1961–71. doi:10.5194/acp-8-6273-2008.

Pinnick, R. G., and H. J. Auvermann. 1979. Response characteristics of knollenberg light-scattering aerosol counters. *J. Aerosol Sci.* 10 (1):55–74. doi:10.1016/0021-8502(79)90136-8.

Prenni, A. J., M. D. Petters, S. M. Kreidenweis, J. Demott, and P. J. Ziemann. 2007. Cloud droplet activation of secondary organic aerosol. *J. Geophys. Res.* 112 (D10223): 1–12. doi:10.1029/2006JD007963..

Pye, H. O. T., B. N. Murphy, L. Xu, N. L. Ng, A. G. Carlton, H. Guo, R. Weber, P. Vasilakos, K. W. Appel, S. H. Budisulistiorini, et al. 2017. On the implications of aerosol liquid water and phase separation for organic aerosol mass. *Atmos. Chem. Phys.* 17 (1):343–69. doi:10.5194/acp-17-343-2017.

Pye, H. O. T., A. Zuend, J. L. Fry, G. Isaacman-VanWertz, S. L. Capps, K. W. Appel, H. Foroutan, L. Xu, N. L. Ng, A. H Goldstein, et al. 2018. Coupling of organic and inorganic aerosol systems and the effect on gas-particle partitioning in the Southeastern United States. *Atmos. Chem. Phys.* 18 (1):357–70. doi:10.5194/acp-2017-623.

Riemer, N., M. West, R. A. Zaveri, and R. C. Easter. 2009. Simulating the evolution of soot mixing state with a particle-resolved aerosol model. *J. Geophys. Res.* 114 (D9): 1–22. doi:10.1029/2008JD011073.

Rui, D., and P. A. Ariya. 2008. The test freezing temperature of C2-C6 dicarboxylic acid: The important indicator for ice nucleation processes. *Sci. Bull.* 53 (17):2685–91. doi:10.1007/s11434-008-0343-0.

von Schneidemesser, E., P. S. Monks, J. D. Allan, L. Bruhwiler, P. Forster, D. Fowler, A. Lauer, W. T. Morgan, P. Paasonen, M. Righi, et al. 2015. Chemistry and the linkages between air quality and climate change. *Chem. Rev.* 115 (10):3856–97. doi:10.1021/acs.chemrev.5b00089.

Schuster, G. L., O. Dubovik, B. N. Holben, and E. E. Clothiaux. 2005. Inferring black carbon content and specific absorption from aerosol robotic network (AERONET) aerosol retrievals. *J. Geophys. Res.* 110 (D10):1–19. doi:10.1029/2004JD004548.

Schwarz, J. P., R. S. Gao, D. W. Fahey, D. S. Thomson, L. A. Watts, J. C. Wilson, J. M. Reeves, M. Darbeheshti, D. G. Baumgardner, G. L. Kok, et al. 2006. Single-particle measurements of midlatitude black carbon and light-scattering aerosols from the boundary layer to the lower stratosphere. *J. Geophys. Res.* 111 (D16):1–15. doi:10.1029/2006JD007076.

Semeniuk, K., and A. Dastoor. 2020. Current state of atmospheric aerosol thermodynamics and mass transfer modeling: A review. *Atmosphere* 11 (2):156–71. doi:10.3390/atmos11020156.

Suda, S. R., M. D. Petters, A. Matsunaga, R. C. Sullivan, P. J. Ziemann, and S. M. Kreidenweis. 2012. Hygroscopicity frequency distributions of secondary organic aerosols. *J. Geophys. Res.* 117 (D04207):1–14. doi:10.1029/2011JD016823..

Suda, S. R., M. D. Petters, G. K. Yeh, C. Strollo, A. Matsunaga, A. Faulhaber, P. J. Ziemann, A. J. Prenni, C. M. Carrico, R. C. Sullivan, et al. 2014. Influence of functional groups on organic aerosol cloud condensation nucleus activity. *Environ. Sci. Technol.* 48 (17):10182–90. doi:10.1021/es502147y.

Thorsen, T. J., R. A. Ferrare, S. Kato, and D. M. Winker. 2020. Aerosol direct radiative effect sensitivity analysis. *Journal of Climate* 33 (14):6119–39. doi:10.1175/JCLI-D-19-0669.1.

Titos, G., A. Cazorla, P. Zieger, E. Andrews, H. Lyamani, M. J. Granados-Muñoz, F. J. Olmo, and L. Alados-Arboledas. 2016. Effect of hygroscopic growth on the aerosol light-scattering coefficient: A review of measurements, techniques and error sources. *Atmos. Environ.* 141:494–507. doi:10.1016/j.atmosenv.2016.07.021.

Wang, W., and M. J. Rood. 2008. Real refractive index: Dependence on relative humidity and solute composition with relevancy to atmospheric aerosol particles. *J. Geophys. Res.* 113 (D23):1–9. doi:10.1029/2008JD010165.

Wang, Y., P.-L. Ma, J. Peng, R. Zhang, J. H. Jiang, R. C. Easter, and Y. L. Yung. 2018. Constraining aging processes of black carbon in the community atmosphere model using environmental chamber measurements. *J. Adv. Model. Earth Syst.* 10 (10):2514–26. doi:10.1029/2018MS001387.

Wexler, A. S., and S. L. Clegg. 2002. E-AIM, extended AIM aerosol thermodynamics model. http://www.aim.env.uea.ac.uk/aim/aim.php.

Wong, J. P. S., J. Liggio, S.-M. Li, A. Nenes, and J. P. D. Abbatt. 2014. Suppression in droplet growth kinetics by the addition of organics to sulfate particles. *J. Geophys. Res. Atmos.* 119 (21):12,222–32. doi:10.1002/2014JD021689.

World Health Organization. 2013. Review of evidence on health aspects of air pollution – REVIHAAP.

Xue, H., A. F. Khalizov, L. Wang, J. Zheng, and R. Zhang. 2009. Effects of dicarboxylic acid coating on the optical properties of soot. *Phys. Chem. Chem. Phys.* 11 (36): 7869–75. doi:10.1039/b916865f.

Yao, X., A. P. S. Lau, M. Fang, C. K. Chan, and M. Hu. 2003. Size distributions and formation of ionic species in atmospheric particulate pollutants in Beijing, China: 2 - Dicarboxylic acids. *Atmos. Environ.* 37 (21):3001–7. doi:10.1016/S1352-2310(03)00256-5.

You, Y., L. Renbaum-Wolff, and A. K. Bertram. 2013. Liquid-liquid phase separation in particles containing organics mixed with ammonium sulfate, ammonium bisulfate, ammonium nitrate or sodium chloride. *Atmos.*

Chem. Phys. 13 (23):11723–34. doi:10.5194/acp-13-11723-2013.

Zanatta, M., P. Laj, M. Gysel, U. Baltensperger, S. Vratolis, K. Eleftheriadis, Y. Kondo, P. Dubuisson, V. Winiarek, S. Kazadzis, et al. 2018. Effects of mixing state on optical and radiative properties of black carbon in the European Arctic. *Atmos. Chem. Phys.* 18 (19):14037–57. doi:10.5194/acp-18-14037-2018.

Zaveri, R. A., R. C. Easter, J. D. Fast, and L. K. Peters. 2008. Model for simulating aerosol interactions and chemistry (MOSAIC). *J. Geophys. Res.* 113 (D13):1–29. doi:10.1029/2007JD008782.

Zhang, C., N. Ma, F. Fan, Y. Yang, J. Größ, J. Yan, L. Bu, Y. Wang, and A. Wiedensohler. 2021. Hygroscopic growth of aerosol particles consisted of oxalic acid and its internal mixture with ammonium sulfate for the relative humidity ranging from 80% to 99.5%. *Atmos. Environ.* 252 (118318):118318–9. doi:10.1016/j.atmosenv.2021.118318.

Zhang, L., J. Y. Sun, X. J. Shen, Y. M. Zhang, H. Che, Q. L. Ma, Y. W. Zhang, X. Y. Zhang, and J. A. Ogren. 2015. Observations of relative humidity effects on aerosol light scattering in the Yangtze River Delta of China. *Atmos. Chem. Phys.* 15 (14):8439–54. doi:10.5194/acp-15-8439-2015.

Zheng, Z., J. H. Curtis, Y. Yao, J. T. Gasparik, V. G. Anantharaj, L. Zhao, M. West, and N. Riemer. 2021. Estimating submicron aerosol mixing state at the global scale with machine learning and earth system modeling. *Earth Space Sci.* 8 (2):1–19. doi:10.1029/2020EA001500.

Zieger, P., R. Fierz-Schmidhauser, E. Weingartner, and U. Baltensperger. 2013. Effects of relative humidity on aerosol light scattering: Results from different European sites. *Atmos. Chem. Phys.* 13 (21):10609–31. doi:10.5194/acp-13-10609-2013.